Chemistry–A European Journal
Research Article
doi.org/10.1002/chem.202203841
Chemistry Europe
European Chemical Societies Publishing
www.chemeurj.org

Light-Triggered Control of Glucocerebrosidase Inhibitors: Towards Photoswitchable Pharmacological Chaperones

Francesca Clemente[+],[a] Maria Giulia Davighi[+],[a] Camilla Matassini,*[a] Francesca Cardona,[a, b] Andrea Goti,[a, b] Amelia Morrone,[c, d] Paolo Paoli,[e] Tomás Tejero,[f] Pedro Merino,[g] and Martina Cacciarini*[a, h]

Abstract: Piperidine-based photoswitchable derivatives have been developed as putative pharmacological chaperones for glucocerebrosidase (GCase), the defective enzyme in Gaucher disease (GD). The structure-activity study revealed that both the iminosugar and the light-sensitive azobenzene are essential features to exert inhibitory activity towards human GCase and a system with the correct inhibition trend (IC_{50} of the light-activated form lower than IC_{50} of the dark form) was identified. Kinetic analyses showed that all compounds are non-competitive inhibitors (mixed or pure) of GCase and the enzyme allosteric site involved in the interaction was identified by means of MD simulations. A moderate activity enhancement of mutant GCase assessed in GD patients' fibroblasts (ex vivo experiments) carrying the most common mutation was recorded. This promising observation paves the way for further studies to improve the benefit of the light-to-dark thermal conversion for chaperoning activity.

Introduction

Gaucher disease (GD), one of the most common lysosomal storage disorders,[1] is characterized by missense mutations in the *GBA* gene, which lead to a total or partial deficiency in the activity of the lysosomal enzyme glucocerebrosidase (GCase).[2] This malfunction causes a harmful accumulation of undegraded glucosylceramide in the lysosome and the onset of several severe symptoms which often involve the central nervous system. One therapeutical strategy for lysosomal storage disorders involves the use of pharmacological chaperones (PC),[3,4] small molecules that can bind to the misfolded protein in the endoplasmic reticulum (ER) promoting its correct folding, which in turn induces its trafficking into the lysosomes. Once in the lysosomes, a rescue of the enzymatic activity occurs. The great majority of PCs identified to date for GCase are competitive inhibitors that bind the active site of the enzyme.

Once the PC-enzyme complex reaches the lysosome, the large amount of stored substrate is supposed to displace the PC allowing the recovery of the enzyme activity.[4d,5] Only few examples of non-competitive inhibitors, that interact with allosteric sites, have been reported as good PCs.[6] In addition, second-generation PCs, known also as allosteric enhancers, have emerged to overcome the drawback of the inhibitory effect. However, their identification has proven to be extremely

[a] *Dr. F. Clemente,[+] M. G. Davighi,[+] Dr. C. Matassini, Prof. Dr. F. Cardona, Prof. A. Goti, Prof. Dr. M. Cacciarini*
Department of Chemistry "U. Schiff"
University of Florence
Via della Lastruccia 3–13, 50019 Sesto F.no (FI) (Italy)
E-mail: camilla.matassini@unifi.it
martina.cacciarini@unifi.it

[b] *Prof. Dr. F. Cardona, Prof. A. Goti*
Associated with LENS
Via N. Carrara 1, 50019 Sesto F.no (FI) (Italy)

[c] *Prof. Dr. A. Morrone*
Laboratory of Molecular Biology of Neurometabolic Diseases
Neuroscience Department, Meyer Children's Hospital
Viale Pieraccini 24, 50139 Firenze (Italy)

[d] *Prof. Dr. A. Morrone*
Department of Neurosciences
Psychology, Drug Research and Child Health
University of Florence
Viale Pieraccini 24, 50139 Firenze (Italy)

[e] *Prof. Dr. P. Paoli*
Department of Experimental and Clinical Biomedical Sciences
University of Florence
Viale Morgagni 50, 50134 Firenze (Italy)

[f] *Prof. Dr. T. Tejero*
Institute of Chemical Synthesis and Homogeneous Catalysis. (ISQCH)
University of Zaragoza
Campus San Francisco, Zaragoza, 50009 (Spain)

[g] *Prof. Dr. P. Merino*
Institute of Biocomputation and Physics of Complex Systems (BIFI)
University of Zaragoza
Campus San Francisco
Zaragoza, 50009 (Spain)

[h] *Prof. Dr. M. Cacciarini*
Department of Chemistry
University of Copenhagen
Universitetsparken 5, DK-2100 Copenhagen Ø (Denmark)

[+] *These Authors contributed equally to this work*

Supporting information for this article is available on the WWW under https://doi.org/10.1002/chem.202203841

hard because it requires a massive screening-based approach.[7,4d]

So far, our efforts have been devoted towards inhibitory-PC candidates, which ideally should have a strong affinity to the target enzyme in the endoplasmic reticulum and a lower binding in the lysosome, favouring the PC-enzyme complex dissociation. A challenging and still under-explored approach that might contribute to this dissociation is the design of stimuli responsive inhibitors. With this aim, PCs engineered with a pH-labile unit have been investigated, taking into account the difference in environmental pH of ER and lysosomes.[8] Once the PC-enzyme complex is transferred inside the lysosome, the more acidic environment induces a structural modification/decomposition of the PC to a low-affinity ligand, therefore leading to the complex dissociation and release of the free enzyme.

An alternative strategy that we have recently proposed[9] consists of tethering thermally reversible photoswitchable moieties to the biologically active unit (Figure 1a), thereby changing the structure and potentially the recognition properties of the system by light irradiation, obtaining two compounds in one (dark isomer and irradiated isomer). A significant difference in inhibitory activity between the two isomers is a first important goal. In this context, maximum benefit is expected when the irradiated isomer ("light-activated") has a stronger binding to the misfolded protein than the thermally relaxed isomer ("time-deactivated" form). Hence, after the recovered protein is transferred from the ER to the lysosome, the inhibitory activity of the PC is suppressed and the enzyme activity can be more efficiently recovered. Thus, an optimized photo-temporal control of the photoswitchable unit is critical, together with a difference in inhibitory activity of the light-activated vs. time-deactivated forms.

We have recently explored photoswitchable inhibitors of GCase,[9] constituted by a dihydroazulene[10] or an azobenzene (AZB)[11] moiety as photoswitchable units and a trihydroxypiperidine as biologically active unit. AZB is a photoswitch that upon light irradiation isomerizes between the *trans* and the *cis* form, with appreciable changes in distance and orientation of the two extremities, and can reversibly undergo thermal- or photo-induced back isomerization at different wavelength (Figure 1c). Based on the observation that the GCase enzyme is responsive to multivalent inhibitors with low valencies,[5g,12] a divalent compound of AZB was also investigated.

Herein, we report the results of further studies involving the following structural modifications of the AZB-based GCase inhibitor candidates: (i) removal of the photoswitchable AZB portion; (ii) replacement of the iminosugar with a simple piperidine; (iii) elongation of the linker between AZB and the trihydroxypiperidine (Figure 1b). The structure-activity relationship as GCase inhibitors, the type of inhibition and the activity as PCs for GCase are presented, discussed and further corroborated by molecular dynamics studies to gain insight into the essential features favouring modulation of GCase activity.

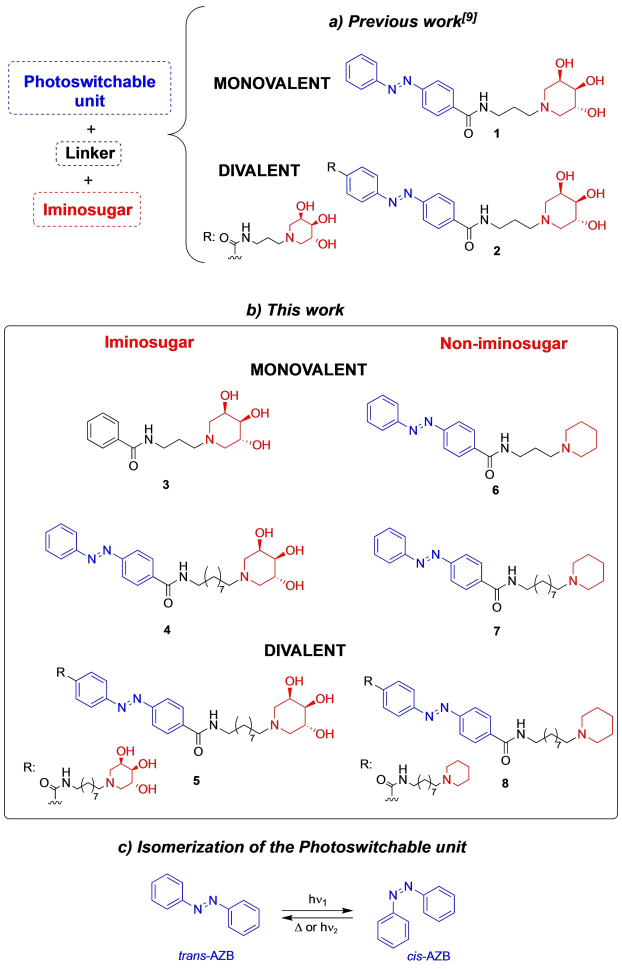

Figure 1. Compounds investigated as GCase inhibitors/PC in previous work (a) and in this work (b). Azobenzene *cis/trans* isomerization (c).

Results and Discussion

Synthesis

Compounds **3**–**8** reported in Figure 1b were selected as useful synthetic targets. The mono- and divalent AZB derivatives **1** and **2** were synthesized according to our previous report.[9] The replacement of the photoswitchable AZB unit on **1** with a phenyl ring was accomplished by reacting the aminotrihydroxypiperidine **9**[13] with benzoyl chloride (**10**) in acetone/water in the presence of K_2CO_3 to give the amide **3** in 72% yield (Scheme 1).

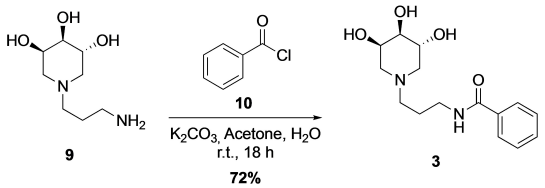

Scheme 1. Synthesis of compound **3**.

Under analogous conditions, 1-(3-aminopropyl)piperidine (**11**)[14] was coupled with 4-phenylazobenzoylchloride (**12**)[15] to yield compound **6** (56%), bearing an unsubstituted piperidine instead of an iminosugar (Scheme 2).

Next, the distance between the iminosugar and the AZB unit was increased by introducing a nine-carbon atom chain (Scheme 3). The amine **13** was prepared in quantitative yield by Staudinger reduction of the azide **14**[5g] and used as a building block to obtain monovalent and divalent compounds. First, **13** was coupled with aroyl chloride **12** in acetone/water in the presence of K_2CO_3 to furnish monovalent **15** (58%), which was deprotected with TFA in CH_2Cl_2 and treated with ammonia affording **4** in 69% yield as exclusive *trans* isomer as attested by ^{1}H NMR spectroscopy (400 MHz). Then, **13** was tethered to the di-aroyl chloride **16**[16] in CH_2Cl_2 in the presence of triethylamine to obtain divalent **17** (66%). Deprotection of **17** with TFA in CH_2Cl_2 gave **5s** (91%, exclusive *trans* isomer by ^{1}H NMR at 400 MHz), as bis-trifluoroacetate salt (Scheme 3), since standard treatments with ammonia did not allow deprotonation.

The non-iminosugar analogues of **4** and **5**, namely **7** and **8**, were also prepared, according to Scheme 4. Hence, amine **18**[17] was reacted in acetone/water in the presence of K_2CO_3 first with **12** to yield monovalent non-iminosugar **7** (59%) and then with **16** to afford divalent non-iminosugar **8** in 20% yield.

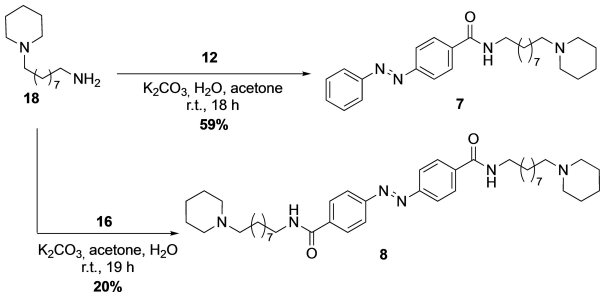

Scheme 4. Synthesis of monovalent compound **7** and divalent compound **8**.

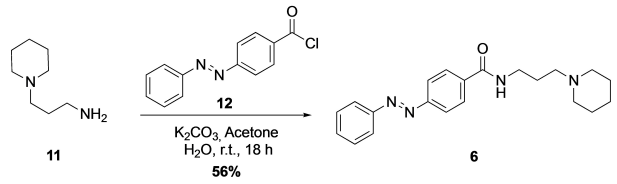

Scheme 2. Synthesis of compound **6**.

The photochemical properties of the newly synthesized iminosugar-photoactive compounds were studied by UV-Vis and NMR spectroscopies. It's worth noting that both compounds **4** and **5** were investigated as their corresponding trifluoroacetate salts **4s** and **5s** (Scheme 3). Indeed **5** was isolated from synthesis as bis trifluoroacetate salt **5s**, and **4**, which was isolated as free amine, had to be transformed into trifluoroacetate salt **4s** due to limited solubility of the free amine. UV-Vis absorption spectra were recorded in 0.2% DMSO in water (i.e., the same medium used for the enzymatic assays), both in the dark and after irradiation with a 340 nm LED lamp, and the specific absorption maxima were found at 325 and 302 nm, respectively for *trans*-**4s** and *trans*-**5s**. The irradiation time of each sample (conc. 10^{-2} M) to reach the photostationary state (*PSS*) was determined until no changes in the UV-Vis spectrum were registered (2–5 h). Then the percentage of

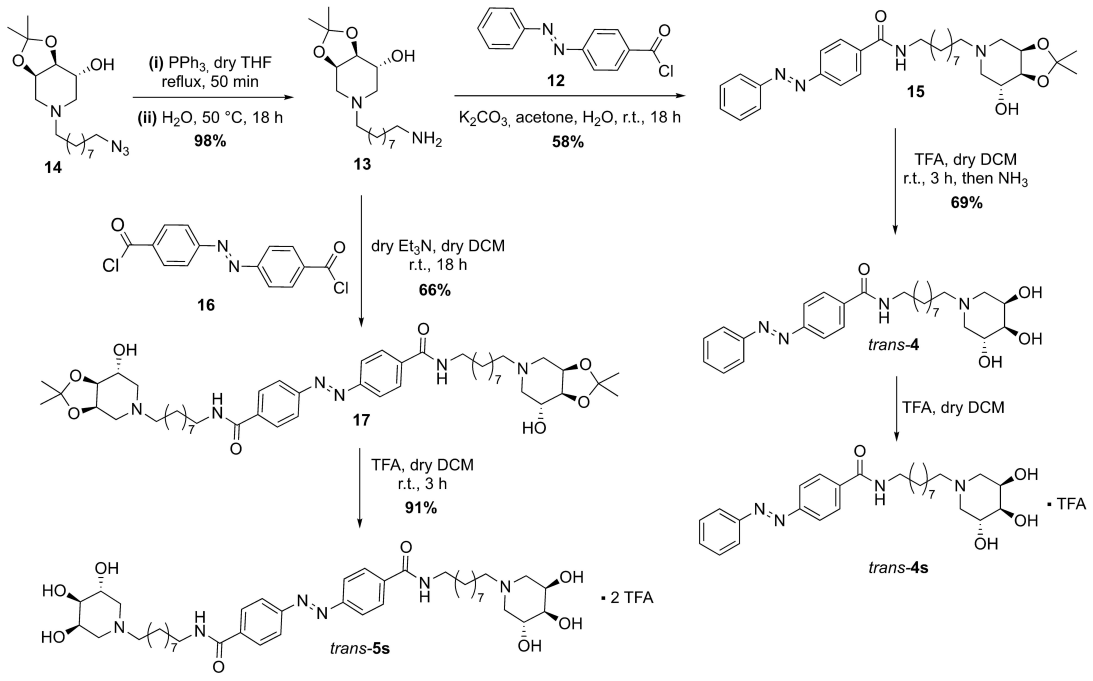

Scheme 3. Synthesis of monovalent *trans*-**4** and divalent *trans*-**5** and corresponding salts. TFA = trifluoroacetic acid.

conversion from *trans* to *cis* was quantified by ^{1}H NMR at 400 MHz, showing that a high percentage of *cis* isomer could be obtained (PSS_{340}-**4s**: 89% *cis*, PSS_{340}-**5s**: 93% *cis*). In both cases we verified that the *cis* isomer has negligible thermal back reaction to the *trans* isomer in the time-frame of the enzymatic assay (1 h at 37 °C).

Biological studies

The mono- and divalent iminosugar-based photoswitchable systems **4s** and **5s** were assayed, before and after irradiation, as GCase inhibitors in human leukocytes from healthy donors at 1 mM. In order to gain insight into the role played by AZB photoswitchable unit, iminosugar and linker, compounds **3**, **6**, **7** and **8** (not irradiated) were also evaluated. The results obtained are compared with those reported for **1**–**2** (Figure 1a) and for control compounds **19**–**22** (Figure 2) in our preliminary communication.[9] For systems with poor to negligible inhibitory activity, only the GCase inhibition percentage at 1 mM is reported (Table 1). Conversely, IC_{50} was calculated and reported in Table 2 (see below) for the best GCase inhibitors (i.e., GCase inhibition at 1 mM ≥ than 95%).

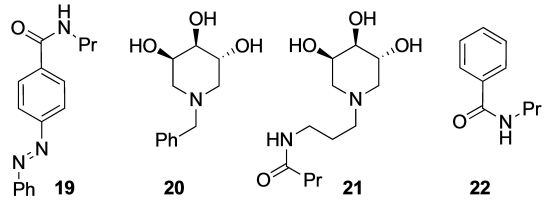

Figure 2. Reference compounds from previous work.[9]

Table 1. GCase inhibition at 1 mM of investigated compounds.

Compound	GCase inhibition at 1 mM [%][a]
Iminosugar-Photoactive	
1	100[b]
2	95[b]
4s	97
5s	100
Non-Iminosugar-Photoactive	
6	58
7	57
8	74[c]
19	18[b]
Iminosugar-Non-Photoactive	
3	62
20	21[b]
21	12[b]
Linker	
22	6[b]

[a] Percentage inhibition of GCase in human leukocyte homogenates from healthy donors; data are mean ± S.D. (n = 3) (see Experimental Section). [b] Ref. [9]. [c] Tested as TFA salt.

Table 2. IC_{50} [μM][a] of dark form (only *trans* isomer) and light-activated (PSS_{340nm})[b] form of **Iminosugar-Photoactive** systems **1**, **2**, **4s** and **5s**.

Compound	PSS_{340nm}	IC_{50}-dark	IC_{50}-light	IC_{50}-dark/IC_{50}-light
1[9]	88% *cis*	15 ± 1	70 ± 3	0.21
2[9]	68% *cis*	35 ± 4	30 ± 2	**1.17**
4s	89% *cis*	24 ± 3	14 ± 2	**1.7**
5s	93% *cis*	7.0 ± 0.1	3.0 ± 0.9	**2.3**

[a] IC_{50} values were determined by measuring GCase activity at different concentrations of each inhibitor in human leukocyte homogenates from healthy donors; data are mean ± S.D. (n = 3). [b] Irradiated at 340 nm for 2–5 h before incubation.

The biological data of control compounds **3** and **6**–**8** (Figure 1b) and **19**–**22** (Figure 2) suggest that the simultaneous presence of iminosugar and AZB moieties is essential for an effective interaction with GCase (Table 1).

The substitution of the trihydroxypiperidine with an unsubstituted piperidine (compounds **6**–**8**) or with a propyl residue (in **19**) resulted in a substantial reduction of GCase inhibition. Likewise, the negligible inhibitory activity towards GCase observed for iminosugar compounds without the AZB moiety (**20**, 21% and **21**, 12%) demonstrates the key role played by this group in the interaction with the target enzyme. A modest 62% inhibitory activity, possibly favoured by hydrophobic or aromatic secondary interactions, was observed in amide **3**, which displays a benzene ring located five atoms away from the iminosugar endocyclic nitrogen. The presence of an aromatic moiety in the inhibitors was previously demonstrated to be beneficial for GCase affinity by some of the authors.[18]

Lastly, the absence of the iminosugar in *N*-propyl benzamide **22** results in lack of inhibition.

We were delighted to observe that all the iminosugar-based photoswitchable systems (light-activated and dark forms) inhibited GCase with percentages ≥ 95% (Table 1) and with IC_{50} values in the micromolar range (3.0 −70.0 μM, Table 2), confirming that the introduction of the photoswitchable moiety does not hamper the inhibition of the GCase enzyme with respect to simply alkylated trihydroxypiperidines.[4a,5e–f,19] Monovalent photoswitchable compound **1**, characterized by a 3-carbon atoms linker between AZB and iminosugar, is a slightly stronger inhibitor than its corresponding 9-carbon atoms analogue **4s** (IC_{50}-dark: 15 vs. 24 μM, Table 2). Conversely, when testing the corresponding *PSS* mixtures, obtained by light irradiation at 340 nm before incubation, we observed for **1** a drop in the inhibitory potency (IC_{50}-light = 70 μM vs. IC_{50}-dark = 15 μM, Table 2), while in the case of **4s** a satisfyingly stronger inhibition was measured on the light irradiated sample (IC_{50}-light = 14 μM vs. IC_{50}-dark = 24 μM, Table 2). These last results are particularly interesting for the purpose of this study, since **4s** exhibited the desired trend with IC_{50}-dark higher than IC_{50}-light. As depicted in Table 2, the IC_{50}-dark/IC_{50}-light ratio = 1.7 makes **4s** a photoswitchable PC candidate.

Among the divalent compounds, elongation of the chain from three to nine carbon atoms between the iminosugar and the AZB moiety produces a remarkable effect on the IC_{50} values. Hence, **5s** is a 5-fold more potent inhibitor than its shorter analogue **2** (IC_{50}-dark: 7.0 vs. 35 μM). Similarly, for the corresponding light irradiated forms *PSS*-**5s** is 10-fold more potent than *PSS*-**2** (IC_{50}-light: 3.0 vs. 30 μM). In this case, the higher percentage of *cis* isomer (93% vs. 68%) established at the *PSS* may play a role on the biological activity. A longer alkyl

chain has previously proven to be beneficial for the enzyme activity according to the trend C12 > C11 > C9 > C8;[19b] here the stronger inhibition might be connected also to the possibility of the divalent inhibitor to interact simultaneously with two GCase enzymes.

The latter feature might be also responsible for the observed positive multivalent effect[20] for *trans*-**5s** with respect to its monovalent counterpart *trans*-**4s**. A positive multivalent effect occurs when the ratio between the relative potency (rp) and the valency (n) is higher than one (rp/n > 1). Thus, in the dark an rp/n = 1.7 is obtained for *trans*-**5s** (7.0 μM) vs. *trans*-**4s** (24 μM). This effect had not been observed previously for *trans*-**2** with respect to *trans*-**1**. Comparing the IC_{50} of light-irradiated forms of mono- and divalent systems with the 9-carbon atom spacer **4s** and **5s** (14 vs. 3.0 μM), an even higher positive multivalent effect is revealed (rp/n = 2.3). Compound **5s**, in its irradiated form (93% *cis*) represents the most potent inhibitor of the whole series of compounds shown in Table 2, with a remarkable IC_{50} = 3.0 μM.

To our delight, the photoactive compounds **4s** and **5s** synthesized in this work showed a reverse and "correct" inhibition trend, with the irradiated forms being better inhibitors than the corresponding dark forms (IC_{50}-dark/IC_{50}-light > 1). Considering that a crucial feature of a PC is to exert a higher binding affinity in the ER than in the lysosome, administering the "light-activated" form (*PSS*) could favour its behaviour as a PC, provided that its reconversion into the "time-deactivated" form (*trans)* occurs in the appropriate time-frame. This would prompt the release of the inhibitor inside the lysosome, leaving the catalytic site available to the natural substrate (see below).

Kinetic analyses

Kinetic analyses were performed with compounds **1**, **2**, **4s** and **5s**. In the case of the more promising compounds **4s** and **5s**, the light irradiated forms were also investigated. In particular, the dependence of the main Michaelis-Menten kinetic parameters (Km and Vmax) vs. the inhibitor concentration was analysed and the results are reported in Table 3.

None of the compounds showed a pure competitive inhibition mode, which was the type of mechanism previously encountered in analogous iminosugar derivatives.[5e–g] However, this behaviour is not unprecedented. Indeed, Compain and co-workers have recently reported that some piperidine iminosugars bearing aromatic moieties such as a triazole-ring behave as non-competitive inhibitors of GCase.[6c]

Compound **1**, bearing the shorter linker between AZB and iminosugar, acts as a pure non-competitive inhibitor (i.e., interacting both with free enzyme and with enzyme-substrate complex), with a Ki value of 14.6 μM. Thus, the presence of the AZB group forces the trihydroxypiperidine out of the active site,[5e–g] suggesting that both trihydroxypiperidine and AZB find an optimal stabilization through hydrogen bonds and hydrophobic interactions in an allosteric site. The conversion from the *trans* to *cis* configuration of the AZB group compels compound **1** to change its interaction mode with the enzyme, resulting in a destabilization of the GCase-inhibitor complex (70 μM vs. 15 μM, Table 2). Unfortunately, it was impossible to determine the Ki value and establish the inhibition type for compound **2** since incoherent results in Km and Vmax variation were found upon increasing its concentration. Conversely, kinetic investigation of compounds **4s** and **5s** and the corresponding light-irradiated forms always revealed a mixed-type inhibition mechanism. The data indicate that the light irradiated and the dark forms show a comparable affinity for the free enzyme (Ki-light and Ki-dark ranging from 4.1 μM to 5.6 μM), while the affinity towards the enzyme-substrate complex is higher for the light-irradiated than for the corresponding dark forms (**4s**: Ki'-light = 10.6 μM vs. Ki'-dark = 71.6 μM; **5s**: Ki'-light = 8.5 μM vs. Ki'-dark = 21.2 μM). In addition, it is worth noting that in the case of Ki'-dark compound **5s** showed a three-fold stronger affinity than **4s**, suggesting a possible role played by the presence of two trihydroxypiperidine units in stabilizing the GCase-inhibitor complex. These results suggest that the presence of substrate bound to the active site of GCase hinders the interaction of the inhibitors with the enzyme (Ki' > Ki).

Table 3. Ki [μM][a] and Ki' [μM][a] of dark forms (only *trans* isomer) and light-activated (PSS_{340nm})[b] forms of **Iminosugar-Photoactive** systems.

System	Ki-dark	Ki'-dark	Ki-light	Ki'-light
1[c]	14.6 ± 0.3	14.6 ± 0.3	n.d.	n.d.
4s[d]	4.4 ± 0.1	71.6 ± 1.6	5.6 ± 1.1	10.6 ± 1.5
5s[d]	4.1 ± 0.4	21.2 ± 4.9	4.3 ± 1.6	8.5 ± 1.3

[a] Determined studying the dependence of the main kinetic parameters (Km and Vmax) from the inhibitor concentration; data are mean ± S.D. (n = 3). [b] Irradiated at 340 nm for 2–5 h before incubation. [c] Non-competitive inhibition. [d] Mixed-type inhibition. n.d. not determined.

Pharmacological Chaperones Activity

The behaviour of the iminosugar-based photoswitchable compounds **1**, **2**, **4s** and **5s** as PCs was assessed by determining the mutant GCase activity enhancement after 4 days co-incubation in fibroblasts from GD patients (ex vivo experiments). The N370S/RecNcil mutation was initially selected as it is one of the most common GCase mutation and known to be responsive to PCs. We previously reported that **1** is able to increase the activity of wild-type GCase by 60% at 50 μM under thermal denaturation conditions, which furnished a preliminary indication of its potential behaviour as a PC.[9] However, once tested in N370S/RecNcil fibroblasts, **1** provided only a negligible enhancement of GCase activity, although at very low concentration (13% at 10 nM, Entry 1, Table 4). We hypothesize that the scarce rescue observed in the ex vivo assay might be ascribed to the conformational change induced by the N370S mutation on the allosteric site (Figure 7, see below), thus reducing the PC effect of **1**.

Compound **2**, despite being a weaker GCase inhibitor than **1**, was the best GCase enhancer of the series increasing the activity of the enzyme up to 50% at 50 μM (Entry 2, Table 4 and

Table 4. GCase activity percentage enhancement on GD fibroblast bearing **N370S/RecNcil** mutation of **Iminosugar-Photoactive** systems.

System	Dark-Fold increase % [μM]	Light-Fold increase % [μM]
1	13% (0.01)	n.d.
2	**46% (50)**	n.d.
4s	11% (10)	12% (0.05)
5s	No increase	11% (1)

Figure 3). This result is not surprising as it is well known[5e–g] that a strong GCase inhibition does not necessarily reflect an effective chaperoning activity, due to other involved factors such as dissociation from the target enzyme and the bioavailability of the compound. Besides, it should be noticed that **2** is a better PC than the simple *N*-octyl trihydroxypiperidine, which showed a 25% GCase rescue at 100 μM.[21] Encouraged by this result, **2** was also tested on GD patient fibroblasts hosting, at homozygous level, the L444P mutation that is responsible for neuropathic form of GD. A valuable 37% GCase activity enhancement was recorded at 10 μM (Figure 3).

Since their affinity towards GCase showed the correct trend (IC_{50}-dark/IC_{50}-light >1, Table 2), the chaperone activity of systems **4s** and **5s** was investigated also on light-irradiated samples. Solutions of **4s** and **5s** in water/DMSO were irradiated at 340 nm (2 h and 5 h, respectively) and immediately diluted in the cell culture medium to obtain the proper final concentrations (10 nM - 100 μM) supplied to the cells. Compound **5s** did not increase GCase activity when only the *trans* isomer was supplied ("dark"), while a 11% GCase rescue at 1 μM was measured on the irradiated sample. In case of compound **4s** the same GCase activity enhancement was recorded on dark and light irradiated samples (11–12%), although displayed at very different concentration (10 μM vs. 50 nM, Table 3).

In summary, compound **2**, which contains a shorter spacer between trihydroxypiperidine and AZB group, was the most effective chaperone among the inhibitors investigated here. Direct comparison with **5s** reveals that the distance between trihydroxypiperidine units is relevant to ensure interaction and stabilization of mutant form of GCase.

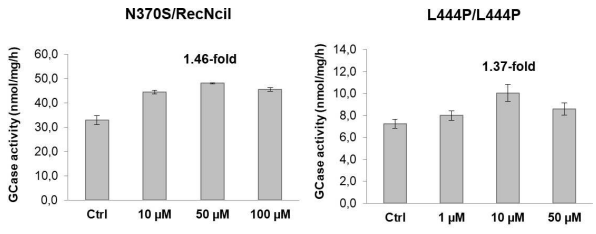

Figure 3. GCase activity in human fibroblasts derived from GD patients bearing N370S/RecNcil (*left*) and L444P/L444P (*right*) mutations, measured after 4 days of incubation without (Ctrl) or with compound **2**.

Molecular Dynamic Studies

The detection of allosteric sites is challenging and their role on the folding, stability and biological properties warrants investigation.[22] GCase activators inducing dimerization have been reported,[23] which in some cases directly increase GCase abundance in patient-derived fibroblast cells.[24] Lieberman et al. discussed the different features of the active site and catalytic mechanism of GCase on the basis of crystallographic studies.[25] Two key features seem to be of crucial importance: (i) the formation of a H-bond between Y313 and E340 which acts as a trigger, activating the enzyme, and (ii) the formation of a helical turn by residues 311–319. Indeed, the Y313–E340 H-bond is not formed in the inactive *apo*-GCase at neutral pH, whereas upon binding with isofagomine (IFG) in the active site, the H-bond is present, triggering the active form of the protein. Conversely, the inactive mutant N370S displays no H-bond between Y313 and E340 with a notable separation of the residues and the *apo*-form shows a different H-bond of Y313 with E235 at low pH (Figure 4). Inactive forms do not present the helical turn at loop 311–319 except for the *apo*-form at neutral pH.[25]

In order to shed light on the possible allosteric control of GCase activity, compounds **1**, **4** and **5** were selected for a computational study. Only *trans*-AZB isomers were considered, due to the in silico instability of *cis*-AZB derivatives. Protonated forms at the piperidine nitrogen atom in both configurations at N were also investigated. Descriptors *cis*-4OH and *trans*-4OH before the compound number designate the configuration at N, where *cis* and *trans* refer to the position of the residue on the N with respect to the hydroxy group at C4 (see Figure MD-S1).[19b]

For the location of binding sites, we used the SiteMap software as implemented in Schrödinger package.[26] The study was carried out with the *apo* form at neutral pH (PDB ID: 2NT1)

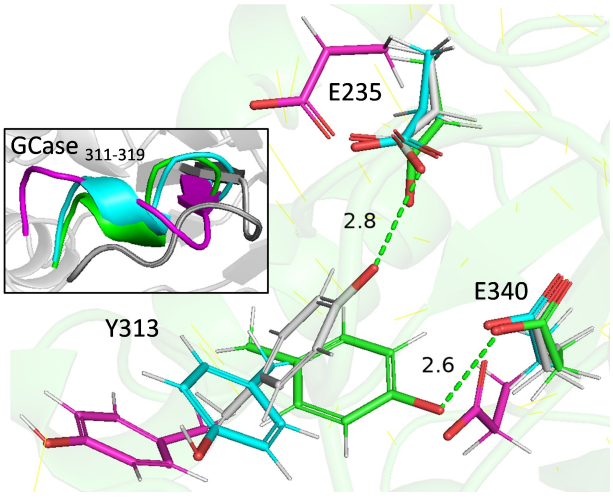

Figure 4. Detail of the trigger involving Y313 in the different forms of GCase. Activation of the enzyme is indicated by the formation of a H-bond between Y313 and E340. *apo*-GCase at low pH is coloured in grey; *apo*-GCase at neutral pH is coloured in cyan; mutant N370S is coloured in magenta and complex GCase-IFG is coloured in green. Square: detail of loop 311–319.

and the complex GCase-IFG (PDB ID: 2NSX), which represents the enzyme bound to a substrate with affinity for the active site. Five binding sites (named as AS1–AS5) were identified, either in the *apo* form and in the complex with IFG. Compounds **1**, **4** and **5** were docked in the binding sites using software Glide as implemented in Schrödinger package (see results in Table S1 and S2).[27] Structures having a Glide score higher than 5 were submitted to MD simulations of at least 500 ns. MD simulations corresponding to complexes with *apo*-GCase showed a low stability and, in most cases, compounds migrate to the active site. Although some stability could be appreciated for compound **1**, no effect on the structure of the protein was observed even after complexing with IFG. Subsequent MD simulations also showed a limited stability of the allosteric ligands. Hence, the approach involving initial binding of allosteric ligand and then complexing with IFG did not provide convincing results. On the other hand, when we carried out MD simulations on ternary complexes of GCase with IFG and allosteric ligands a significant stability for compounds *trans*-4OH-**1H**$^+$ and *trans*-4OH-**4H**$^+$ was observed. In fact, it seems that binding of *trans*-4OH-**1H**$^+$ promotes the opening of the active site pocket even in the presence of IFG (Figure 5). After just 10 ns, the H-bond still survives but the region 311–319 has lost its secondary structure. At 100 ns the loop becomes, temporarily, helical and the enzyme activity is turned off by the displacement of Y313. E340 gives an H-bond with IFG, which remains in its binding site. Finally, after 400 ns also the loop has definitely lost the secondary structure and the enzyme its activity.

Compound *trans*-4OH-**4H**$^+$ bound in the same allosteric site found for *trans*-4OH-**1H**$^+$ close to loop 311–319 and not far from the active site, albeit interacting with different portions of the inhibitor. Essentially, the same effects were observed (Figure 6). Initially, the H-bond is formed between Y313 and E340 and the loop 311–319 has a helical structure. After 300 ns, the H-bond is lost and the loop has lost the secondary structure. As for *trans*-4OH-**1H**$^+$, a H-bond between E340 and IFG is formed inducing a change of position for IFG. At 500 ns, the allosteric ligand *trans*-4OH-**4H**$^+$ leaves the site and the loop recovers the secondary structure. When the allosteric site is free at 1 microsecond, the H-bond between Y313 and E340 is recovered, even though that between E340 and IFG is conserved.

It can be concluded that for both compounds **1** and **4** the allosteric binding is reversible and has a temporary effect, as inferred from MD simulations. The weak bonding of this ligand may be consistent with the observed variation of inhibitory activity on a subtle structural change such as the *trans/cis* conversion.

In summary, computational studies based on MD simulations located an allosteric area close to the active site, where compounds **1** and **4** can bind upon protonation, causing effects which affect the activation of the enzyme GCase (Figure 7).

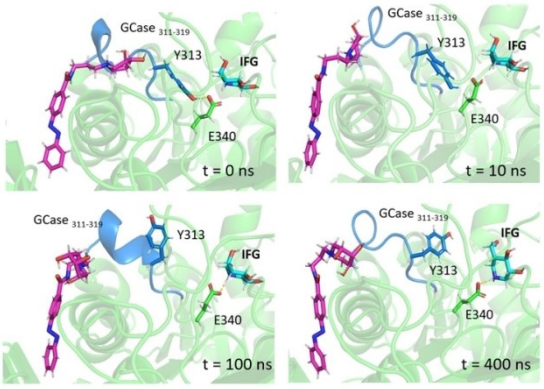

Figure 5. Snapshots corresponding to MD simulations of allosteric binding of *trans*-4OH-**1H**$^+$ to GCase-IFG complex. Compound *trans*-4OH-**1H**$^+$ is given in magenta; IFG in cyan; loop 311–319 and residues belonging to it in marine blue; proteins are shown in green.

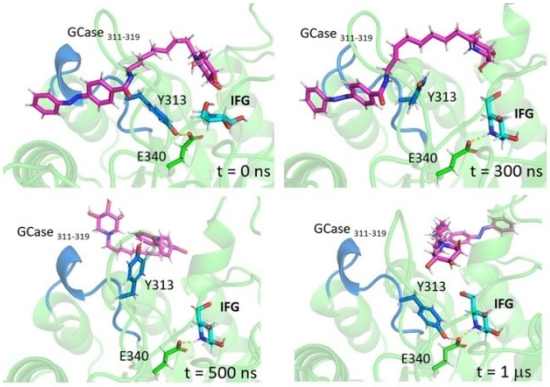

Figure 6. Snapshots corresponding to MD simulations of allosteric binding of *trans*-4OH-**4H**$^+$ to GCase-IFG complex. Compound *trans*-4OH-**4H**$^+$ is given in magenta; IFG in cyan; loop 311–319 and residues belonging to it in marine blue; proteins are shown in green.

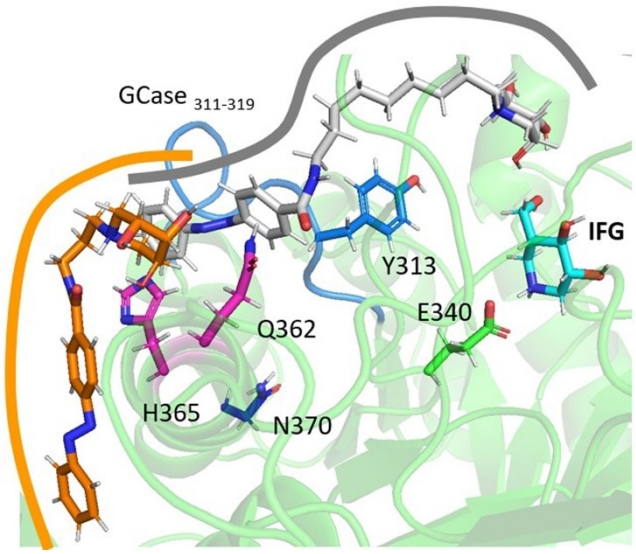

Figure 7. Allosteric site found for GCase. Ligands *trans*-4OH-**1H**$^+$ (orange) and *trans*-4OH-**4H**$^+$ (grey) are shown in the positions able to trigger structural variations. IFG is shown in cyan, GCase residues showing interactions with both ligands are shown in magenta.

Aminoacids Q362 and H365, next to the N370S mutation investigated in ex vivo tests, are common residues to the two sites in which *trans*-4OH-**1H**$^+$ and *trans*-4OH-**4H**$^+$ bind, having interactions with the ligands (Figure 7).

Conclusion

We performed a structure-activity study of light responsive iminosugar-azobenzene derivatives that act as GCase inhibitors in the micromolar range. Both trihydroxypiperidine and AZB units have been recognized as key components for optimization of enzyme inhibition. Determining the inhibition mechanism revealed that none of the compounds showed a pure competitive inhibition mode, previously established in analogous iminosugar derivatives. Conversely, either a non-competitive or a mixed inhibition were found, indicating that these inhibitors bind to allosteric rather than to the active site. Preliminary docking studies, together with MD simulations on ternary complexes of GCase with IFG and allosteric ligands, allowed us to identify the allosteric site involved in the interaction.

Progress in the development of photoswitchable inhibitor systems has been made given our success in identifying photoactive pairs, which show stronger affinity towards GCase in the light irradiated form than in the dark form. The structural change of the molecule induced by light should maximize the pharmacological chaperoning activity with respect to the inhibitory behaviour when these molecules reach the lysosomes. However, when we tested the irradiated forms of compounds **4s** and **5s** in fibroblasts derived from Gaucher patients bearing the N370S/RecNcil mutations, only a slight increase (around 10%) in mutated GCase activity was observed. Analogously, for the dark-form of **1**, **4s** and **5s**, the GCase enhancement was limited or absent. The highest enhancement of enzyme activity was found for compound **2** (46%) in fibroblasts derived from Gaucher patients bearing the N370S/RecNcil mutations. In addition, compound **2** was also able to enhance mutated GCase activity in fibroblasts bearing the homozygous L444P mutation, a cell line resistant to most PCs, by 37%. Notably, compound **2** is a less potent GCase inhibitor than **1**, **4s** and **5s**, but it corresponds to the best chaperone on cell lines. These data suggest that the mutated GCase refolding induced by the interaction with the inhibitor does not stabilize the enzyme sufficiently to produce a significant PC effect, as it can be for non-competitive inhibitors, and that the biological response to light-to-dark conversion is not yet effective. Further improvements for PC candidates for Gaucher disease shall rely on structural modification of the photoswitchable units to optimize the back conversion time frame and amplify the difference in affinity of the two species (light vs. dark).

Experimental Section

General Procedures: Commercial reagents were used as received. All reactions were carried out under magnetic stirring and monitored by TLC on 0.25 mm silica gel plates (Merck F254). Column chromatographies were carried out on Silica Gel 60 (32–63 μm) or on silica gel (230–400 mesh, Merck). Yields refer to spectroscopically and analytically pure compounds unless otherwise stated. Melting points were obtained with a Stuart Scientific melting point apparatus and are uncorrected. Elemental analyses were performed with a Thermoscientific FlashSmart Elemental Analyzer CHNS/O. ^{1}H NMR and ^{13}C NMR spectra were recorded on a Varian Gemini 200 MHz, a Varian Mercury 400 MHz or on a Varian INOVA 400 MHz instrument at 25 °C. Chemical shifts are reported relative to $CDCl_3$ (^{13}C: $\delta = 77.0$ ppm, ^{1}H: 7.26 ppm), or to CD_3OD (^{13}C: $\delta = 49.0$ ppm, ^{1}H: 3.31 ppm). Integrals are in accordance with assignments, coupling constants are given in Hz. For detailed peak assignments 2D spectra were measured (COSY, HSQC). IR spectra were recorded with a IRAffinity-1S SHIMADZU or IRAffinity-1 SHIMADZU system spectrophotometers. Optical rotation measurements were performed on a JASCO DIP-370 polarimeter. High Resolution Mass spectrometry (HRMS) were recorded with an ESP-MALDI-FT-ICR spectrometer equipped with a 7 T magnet (calibration of the instrument was done with NaTFA cluster ions) using Electrospray Ionization (ESI). UV-Vis absorption spectra were recorded on a Varian Cary50 Bio UV-Vis spectrometer at 25 °C and quartz cuvettes with 1-cm light path were used. Irradiation experiments were performed using ThorLabs M340 L4 LED lamp for wavelength of 340 nm. Reaction and purification of light sensitive materials were performed shading the flask or the column with aluminium foil. Compounds **9**, **12**, **14**, and **16** were synthesized following previously reported procedures. Amine **11** and **18**, already described in literature as ammonium salts, were prepared via slightly modified procedures (see Supporting Information). For practical reasons the assignment of H and C atoms in NMR characterizations reflects the numbering of chemical structures in the Supporting Information.

Synthetic procedures

3: A solution of benzoyl chloride **10** (85 mg, 0.60 mmol) in acetone (4 mL) was added to a solution of amine **9**[13] (110 mg, 0.58 mmol) and K_2CO_3 (35 mg, 0.25 mmol) in H_2O (1 mL). The reaction mixture was stirred at room temperature for 18 h until the disappearance of **9** was assessed by a TLC control (DCM/MeOH/NH_4OH (6%) 5:1:0.1). The mixture was concentrated under vacuum and then the crude was purified by FCC in the dark (SiO_2, DCM/MeOH/NH_4OH (6%) 4:1:0.1) to give **3** (123 mg, 0.42 mmol, 72%) as a colourless oil. $R_f = 0.18$ (DCM/MeOH/NH_4OH (6%) 5:1:0.1); $[\alpha]_D^{23} = -22.6$ (c = 1 in MeOH); ^{1}H NMR (400 MHz, CD_3OD): $\delta = 7.86$–7.81 (m, 2H; Ar–H), 7.55–7.43 (m, 3H; Ar–H), 3.91 (dt, $J = 3.0$, 5.5 Hz, 1H; H-3), 3.80 (td, $J = 4.0$, 7.8 Hz, 1H; H-5), 3.50–3.38 (m, 3H, H-4; CH_2-9), 2.91–2.70 (m, 2H; Ha-2, Ha-6), 2.48 (t, $J = 7.1$ Hz, 2H; CH_2-7), 2.36–2.25 (m, 1H; Hb-2), 2.18–2.02 (m, 1H; Hb-6), 1.87–1.77 (m, 2H; CH_2-8); ^{13}C NMR (100 MHz, CD_3OD): $\delta = 170.1$, 135.6, 132.6, 129.5 (2 C), 128.3 (2 C), 75.3, 69.6, 69.2, 58.2, 57.7, 56.6, 39.4, 27.1. IR (neat): $\tilde{\nu} =$ 3300 (br), 2928 (w), 2816 (w), 1634 (vs), 1576 (m), 1539 (vs), 1489 (m), 1310 (s), 1066 (vs), 837 (s) cm^{-1}. HRMS (ESP+): *m/z* calcd for $C_{15}H_{22}N_2O_4$: 295.16523 $[M+H]^+$; found: 295.16525.

6: A solution of diazo acyl chloride **12**[15] (47 mg, 0.19 mmol) in acetone (1.4 mL) was added to a solution of amine **11**[14] (26 mg, 0.18 mmol) and K_2CO_3 (11 mg, 0.08 mmol) in H_2O (0.4 mL). The reaction mixture was stirred at room temperature

for 18 h until the disappearance of **11** was assessed by a TLC control (DCM/MeOH/NH_4OH (6%) 5:1:0.1). The mixture was concentrated under vacuum and then the crude was purified by FCC in the dark (SiO_2, DCM/MeOH/NH_4OH (6%) 10:1:0.2) to give **6** (36 mg, 0.10 mmol, 56%) as an orange solid. R_f = 0.32 (DCM/MeOH/NH_4OH (6%) 10:1:0.1); m.p. = 108-110 °C; ^{1}H NMR (400 MHz, $CDCl_3$): δ = 8.90 (br s, 1H; N*H*), 8.02–7.89 (m, 6H; Ar–H), 7.56–7.45 (m, 3H; Ar–H), 3.64–3.54 (m, 2H; CH_2-9), 2.57–2.51 (m, 2H; CH_2-7), 2.50–2.26 (m, 4H; CH_2-2, CH_2-6), 1.83–1.73 (m, 2H; CH_2-8), 1.63-1.54 (m, 4H; CH_2-3, CH_2-5), 1.53–1.39 (m, 2H; CH_2-4); ^{13}C NMR (100 MHz, $CDCl_3$): δ = 166.6, 154.1, 152.6, 136.9, 131.6, 129.2 (2 C), 128.2 (2 C), 123.1 (2 C), 122.8 (2 C), 59.6, 54.9 (2 C), 41.6, 26.1 (2 C), 24.3, 23.9; IR (neat): $\tilde{\nu}$ = 3314 (m), 2932 (s), 2853 (w), 2770 (m), 1626 (vs), 1533 (vs), 1495 (m), 1141 (m), 1310 (m), 1294 (s), 1267 (m), 1153 (m), 1099 (m), 918 (w) 858 (vs) cm^{-1}; UV-Vis ($CHCl_3$): λ_{max} (ε) = 327 (3.45×10^4), 443 nm (shoulder,1.52×10^3 mol^{-1}dm^{3}cm^{-1}); HRMS (ESP+): *m/z* calcd for $C_{21}H_{26}N_4O$: 351.21794 $[M+H]^+$; found: 351.21828.

13: PPh_3 (65 mg, 0.25 mmol) was added to a solution of **14**[6] (70 mg, 0.21 mmol) in dry THF (3.4 mL), and the mixture was stirred at reflux for 50 minutes until water (7 μL) was added and the reaction was left at 50 °C for 18 h. The disappearance of the starting material **14** was assessed via TLC (CH_2Cl_2/MeOH/NH_4OH (6%) 5:1:0.1) and the reaction was concentrated under vacuum. The crude residue was purified by flash column chromatography on silica gel (gradient eluent CH_2Cl_2/MeOH/NH_4OH (6%) from 10:1:0.1 to 2:1:0.1) to give **13** (64 mg, 0.20 mol, 98%) as a colourless oil. R_f = 0.08 (CH_2Cl_2/MeOH/NH_4OH (6%) 5:1:0.1); $[\alpha]_D^{22}$ = +9.7 (c = 1 in $CHCl_3$); ^{1}H NMR (400 MHz, $CDCl_3$): δ = 4.25 (q, *J* = 6.0 Hz, 1H; H-3), 4.02–3.96 (m, 1H; H-4), 3.92–3.86 (m, 1H; H-5), 2.71–2.61 (m, 3H; Ha-2, CH_2-15), 2.56 (dd, *J* = 2.6, 11.6 Hz, 1H; Ha-6), 2.47–2.28 (m, 4H; Hb-2, Hb-6, CH_2-7), 2.10 (br s, 2H; NH_2), 1.48 (s, 3H; Me), 1.46–1.36 (m, 4H; CH_2-8, CH_2-14), 1.33 (s, 3H; Me), 1.30–1.20 (m, 10H; CH_2-9, CH_2-10, CH_2-11, CH_2-12, CH_2-13); ^{13}C NMR (100 MHz, $CDCl_3$): δ = 109.3, 77.4, 72.4, 67.7, 57.9, 55.9, 55.8, 42.2, 33.7 (2 C), 29.6, 29.5, 29.5, 28.4, 27.4, 26.9, 26.5; IR ($CHCl_3$): $\tilde{\nu}$ = 3851 (w), 3741 (w), 3579 (w), 2932 (vs), 2850 (s), 1666 (br), 1509 (w), 1457 (w), 1380 (m), 1254 (m), 1067 (s) cm^{-1}; HRMS (ESP+): *m/z* calcd for $C_{17}H_{34}N_2O_3$: 315.26422 $[M+H]^+$; found: 315.26450.

15: A solution of diazo acyl chloride **12**[15] (49 mg, 0.20 mmol) in acetone (2 mL) was added to a solution of amine **13** (60 mg, 0.19 mmol) and K_2CO_3 (11 mg, 0.08 mmol) in H_2O (0.5 mL). The reaction mixture was stirred at room temperature for 18 h until the disappearance of **13** was assessed by a TLC control (DCM/MeOH/NH_4OH (6%) 10:1:0.1). The mixture was concentrated under vacuum and then the crude was purified by FCC in the dark (SiO_2, DCM/MeOH/NH_4OH (6%) 25:1:0.1) to give **15** (58 mg, 0.11 mmol, 58%) as an orange solid. R_f = 0.34 (DCM/MeOH/NH_4OH (6%) 10:1:0.1); m.p. = 91–93 °C; $[\alpha]_D^{24}$ = +13.4 (c = 0.65 in $CHCl_3$); ^{1}H NMR (400 MHz, $CDCl_3$): δ = 7.98-7.86 (m, 6H; Ar–H), 7.57–7.44 (m, 3H; Ar–H), 6.36 (t, *J* = 5.4 Hz, 1H; N*H*), 4.28 (q, *J* = 6.0 Hz, 1H; H-3), 4.05 (t, *J* = 4.3 Hz, 1H; H-4), 3.96-3.91 (m, 1H; H-5), 3.46 (q, *J* = 6.8 Hz, 2H; CH_2-15), 3.03–2.84 (m, 1H; O*H*), 2.75 (dd, *J* = 6.0, 11.8 Hz, 1H; Ha-2), 2.59–2.53 (m, 1H; Ha-6), 2.53–2.47 (m, 1H; Hb-6), 2.42–2.30 (m, 3H; Hb-2, CH_2-7), 1.62 (quint, *J* = 7.0 Hz, 2H; CH_2-14), 1.49 (s, 3H; Me), 1.47–1.41 (m, 2H; CH_2-8), 1.40–1.22 (m, 13H; Me, CH_2-9, CH_2-10, CH_2-11, CH_2-12, CH_2-13); ^{13}C NMR (100 MHz, $CDCl_3$): δ = 166.9, 154.2, 152.6, 136.7, 131.7, 129.3 (2 C), 128.0 (2 C), 123.1 (2 C), 123.0 (2 C), 109.4, 76.8, 72.1, 67.6, 57.9, 55.9, 55.5, 40.4, 29.8, 29.5, 29.5, 29.3, 28.4, 27.4, 27.1, 26.9, 26.5; IR (neat): $\tilde{\nu}$ = 3333 (br), 2928 (s), 2851 (s), 1634 (vs), 1539 (s), 1470 (m), 1379 (m), 1296 (m), 1242 (m), 1219 (s), 1148 (m), 1057 (vs), 928 (m), 858 (vs) cm^{-1}; UV-Vis ($CHCl_3$): λ_{max} (ε) = 326 (3.63×10^4), 448 nm (shoulder, 8.58×10^2 mol^{-1}dm^{3}cm^{-1}); HRMS (ESP+): *m/z* calcd for $C_{30}H_{42}N_4O_4$: 523.32788 $[M+H]^+$; found: 523.32763.

trans-**4**: A solution of **15** (39 mg, 0.08 mmol) in dry DCM (1.2 mL) was left stirring with TFA (127 μL, 1.65 mmol) at room temperature for 3 h until the disappearance of starting material was assessed by a TLC control (DCM/MeOH/NH_4OH (6%) 20:1:0.1). Then, the crude mixture was concentrated and the crude residue was purified by FCC in the dark (SiO_2, DCM/MeOH/NH_4OH (6%) 10:1:0.1) to give the *trans* isomer **4** (25 mg, 0.05 mmol, 69%) as established from ^{1}H NMR at 400 MHz, as an orange solid. R_f = 0.16 (DCM/MeOH/NH_4OH (6%) 10:1:0.1); m.p. = 145–147 °C; $[\alpha]_D^{26}$ = −3.2 (c = 0.5 in MeOH); ^{1}H NMR (400 MHz, CD_3OD/$CDCl_3$ 4/1): δ = 8.01–7.89 (m, 6H; Ar–H), 7.58–7.48 (m, 3H; Ar–H), 3.91–3.87 (m, 1H; H-3), 3.79 (td, *J* = 4.0 Hz, 1H; H-5), 3.43–3.35 (m, 3H; H-4, CH_2-15), 2.89–2.73 (m, 2H; Ha-2, Ha-6), 2.43–2.33 (m, 2H; CH_2-7), 2.28 (br d, *J* = 11.2 Hz, 1H; Hb-2), 2.15–2.01 (m, 1H; Hb-6), 1.64 (quint, *J* = 7.3 Hz, 2H; CH_2-14), 1.48 (quint, *J* = 7.4 Hz, 2H; CH_2-8), 1.42–1.24 (m, 10H; CH_2-9, CH_2-10, CH_2-11, CH_2-12, CH_2-13); ^{13}C NMR (50 MHz, $CDCl_3$): δ = 169.0, 155.2, 153.6, 137.6, 132.5, 130.1, 129.1, 123.8, 123.5, 75.0, 69.2, 68.8, 59.0, 57.9, 57.3, 41.0, 30.4, 30.2, 28.4, 27.9, 27.2 Some carbons are missing due to overlap; IR (neat): $\tilde{\nu}$ = 3316 (br), 2926 (s), 2851 (s), 1632 (vs), 1533 (vs), 1470 (w), 1296 (s), 1221 (m), 1055 (vs), 856 (s) cm^{-1}; UV-Vis (0.1% DMSO in water): λ_{max} (ε) = 325 nm (1.21×10^4 mol^{-1}dm^{3}cm^{-1}); HRMS (ESP+): *m/z* calcd for $C_{27}H_{38}N_4O_4$: 483.29658 $[M+H]^+$; found: 483.29645. *trans*-**4** showed extremely low solubility into the assay medium and therefore was transformed into its trifluoromethanesulfonate salt *trans*-**4s**. Thus *PSS*-**4s** was obtained after irradiation of a 10^{-2} M solution of *trans*-**4s** in 50% DMSO in water with 340 nm LED lamp for 2 h. A *cis/trans* ratio of 7.7/1 (89% *cis*) was determined for *PSS*-**4s** from ^{1}H NMR in D_2O with 5% DMSO at 400 MHz. *PSS*-**4s**: UV-Vis (0.1% DMSO in water): λ_{max} (ε) = 323 (1.03×10^4), 428 nm (shoulder, 1.21×10^3 mol^{-1}dm^{3}cm^{-1}); selected signals of the AZB moiety for determination of *PSS*: ^{1}H NMR (400 MHz, D_2O with 5% DMSO): δ = 7.52–7.46 (m, 2H; Ar–H), 7.19–7.06 (m, 3H; Ar–H), 6.88–6.82 (m, 2H; Ar–H), 6.81–6.75 (m, 2H; Ar–H).

17: To a solution of amine **13** (58 mg, 0.18 mmol) in dry DCM (2 mL), dry NEt_3 (39 μL, 0.28 mmol) and **16**[15] (28 mg, 0.09 mmol) were added. The reaction mixture was stirred at room temperature for 18 h until the disappearance of **13** was assessed by a TLC control (DCM/MeOH/NH_4OH (6%) 8:1:0.1). The mixture was concentrated under vacuum and then the crude was purified by FCC in the dark (SiO_2, AcOEt/MeOH/NH_4OH (6%) 10:1:0.1) to give **17** (52 mg, 0.06 mmol, 66%) as an orange oil. R_f = 0.24 (AcOEt/MeOH/NH_4OH (6%) 10:1:0.1); $[\alpha]_D^{24}$ = +9.8 (c = 0.5 in $CHCl_3$); ^{1}H NMR (400 MHz, $CDCl_3$): δ = 7.99–7.88 (m, 8H; Ar–H), 6.31 (t, 2H; N*H*), 4.30 (q, *J* = 6.1 Hz, 2H;

H-3, H-3′), 4.06 (t, $J=4.4$ Hz, 2H; H-4, H-4′), 3.97–3.92 (m, 2H; H-5, H-5′), 3.48 (q, $J=6.7$ Hz, 4H; CH_2-15, CH_2-15′), 2.78 (dd, $J=6.0$, 11.7 Hz, 2H; Ha-2, Ha-2′), 2.60–2.49 (m, 4H; CH_2-6, CH_2-6′), 2.44–2.31 (m, 6H; Hb-2, Hb-2′, CH_2-7, CH_2-7′), 1.69–1.60 (m, 4H; CH_2-14, CH_2-14′), 1.50 (s, 6H; 2xMe), 1.49–1.43 (m, 4H; CH_2-8, CH_2-8′), 1.38–1.24 (m, 26H; CH_2-9, CH_2-10, CH_2-11, CH_2-12, CH_2-13, CH_2-9′, CH_2-10′, CH_2-11′, CH_2-12′, CH_2-13′, 2xMe); ^{13}C NMR (100 MHz, $CDCl_3$): $\delta=166.8$, 154.1, 137.2, 128.0, 123.3, 109.5, 76.7, 72.1, 67.5, 57.9, 55.9, 55.4, 40.4, 29.8, 29.5, 29.5, 29.3, 28.4, 27.4, 27.1, 26.9, 26.5 Some carbons are missing due to overlap; IR (neat): $\tilde{\nu}=3308$ (br), 2926 (s), 2853 (m), 1632 (vs), 1537 (vs), 1456 (w), 1379 (m), 1296 (m), 1242 (m), 1217 (s), 1144 (m), 1057 (vs), 860 (vs) cm^{-1}; UV-Vis ($CHCl_3$): λ_{max} (ε) = 322 (3.43×10^4), 455 nm (shoulder, 2.82×10^2 $mol^{-1}dm^3cm^{-1}$); HRMS (ESP+): *m/z* calcd for $C_{48}H_{74}N_6O_8$: 863.56409 $[M+H]^+$; found: 863.56442.

trans-**5s**: A solution of **17** (40 mg, 0.05 mmol) in dry DCM (1 mL) was left stirring with TFA (78 μL, 1.01 mmol) at room temperature for 3 h until the disappearance of starting material was assessed by a TLC control (DCM/MeOH/NH_4OH (6%) 10:1:0.1). Then, the crude mixture was concentrated, and the crude residue was purified by FCC in the dark (SiO_2, DCM/MeOH/NH_4OH (6%) 4:1:0.1) to give the fully *trans* isomer salt **5s** (43 mg, 0.04 mmol, 91%) as established from ^{1}H NMR at 400 MHz as an orange oil. $R_f=0.09$ (DCM/MeOH/NH_4OH (6%) 4:1:0.1); ^{1}H NMR (400 MHz, CD_3OD): $\delta=8.04$–7.97 (m, 8H; Ar–H), 4.20–4.11 (m, 2H; H-3, H-3′), 4.05–4.00 (m, 2H; H-5, H-5′), 3.89 (br s, 2H; H-4, H-4′), 3.41 (t, $J=7.1$ Hz, 4H; CH_2-15, CH_2-15′), 3.29–2.93 (m, 12H; CH_2-2, CH_2-6, CH_2-7, CH_2-2′, CH_2-6′, CH_2- 7′), 1.81–1.61 (m, 8H; CH_2-8, CH_2-14, CH_2-8′, CH_2-14′), 1.44-1.35 (m, 20H; CH_2-9, CH_2-10, CH_2-11, CH_2-12, CH_2-13, CH_2-9′, CH_2-10′, CH_2-11′, CH_2-12′, CH_2-13′); ^{13}C NMR (^{13}C 100 MHz and gHSQC ^{1}H/^{13}C 100/400 MHz, CD_3OD): $\delta=169.1$, 163.0 ($^2J_{C\text{-}F}=34.3$ Hz; CF_3COO), 155.4, 138.4, 129.4, 124.0, 118.3 ($^1J_{C\text{-}F}=291.3$ Hz; CF_3), 67.7, 63.8, 58.2, 52.8, 52.3, 41.1, 30.4, 30.3, 30.2, 30.1, 28.0, 27.5, 25.0; ^{19}F NMR (376 MHz, CD_3OD): $\delta=76.9$; IR (neat): $\tilde{\nu}=3300$ (br), 2926 (m), 2854 (m), 1668 (vs), 1632 (vs), 1539 (s), 1435 (m), 1317 (w), 1298 (w), 1200 (vs), 1180 (vs), 1128 (vs), 1013 (m) cm−1; UV-Vis (0.2% DMSO in water): λ_{max} (ε) = 302 nm (1.21×10^4 $mol^{-1}dm^3cm^{-1}$); HRMS (ESP+): *m/z* calcd for $C_{42}H_{66}N_6O_8$: 783.50149 $[M+H]^+$; found: 783.50084; elemental analysis calcd (%) for $C_{42}H_{66}N_6O_8\cdot2(CF_3COOH)$: C 54.65, H 6.78, N 8.31; found: C 54.96, H 7.16, N 8.44. *PSS*-**5s** was obtained after irradiation of a 10^{-2} M solution of *trans*-**5s** in 50% DMSO in water with 340 nm LED lamp for 5 h. A *cis/trans* ratio of 13.2/1 (93% *cis*) was determined for *PSS*-**5s** from ^{1}H NMR in D_2O with 5% DMSO at 400 MHz. *PSS*-**5**: UV-Vis (0.2% DMSO in water): λ_{max} (ε) = 296 (1.32×10^4), 423 nm (shoulder, 2.54×10^3 $mol^{-1}dm^3cm^{-1}$); selected signals of the AZB moiety for determination of *PSS*: ^{1}H NMR (400 MHz, D_2O with 5% DMSO): $\delta=7.48$ (d, 4H, $J=8.4$ Hz; Ar–H), 6.86 (d, 4H, $J=8.4$ Hz; Ar–H). It's worth noting that H-2, H-2′, H-4, H-4′, H-6, H-6′, H-7 and H-7′ displayed significant lower integral values than the other protons and C-3, C-4 and C-5 were not visible from the standard ^{13}C spectrum, but were identified in the gHSQC. Therefore, to unequivocally determine the structure of **5s**, the compound was peracetylated and fully characterized (See Supporting Information).

7: A solution of diazo acyl chloride **12** (60 mg, 0.25 mmol) in acetone (2 mL) was added to a solution of amine **18** (53 mg, 0.24 mmol) and K_2CO_3 (14 mg, 0.10 mmol) in H_2O (0.5 mL). The reaction mixture was stirred at room temperature for 18 h until the disappearance of **18** was assessed by a TLC control (DCM/MeOH/NH_4OH (6%) 10:1:0.1). The mixture was concentrated under vacuum and then the crude was purified by FCC in the dark (SiO_2, DCM/MeOH/NH_4OH (6%) 10:1:0.2) to give **7** (60 mg, 0.14 mmol, 59%) as an orange solid. $R_f=0.34$ (DCM/MeOH/NH_4OH (6%) 10:1:0.2); m.p. = 103–105 °C; ^{1}H NMR (400 MHz, $CDCl_3$): δ = 7.97–7.85 (m, 6H; Ar–H), 7.55–7.44 (m, 3H; Ar–H), 6.41 (br s, 1H; N*H*), 3.45 (q, $J=6.3$ Hz, 2H; CH_2-15), 2.46–2.32 (m, 4H; CH_2-2, CH_2-6), 2.28 (t, $J=7.7$ Hz, 2H; CH_2-7), 1.66–1.55 (m, 6H; CH_2-3, CH_2-5, CH_2-14), 1.52-1.22 (m, 14H; CH_2-4, CH_2-8, CH_2-9, CH_2-10, CH_2-11, CH_2-12, CH_2-13); ^{13}C NMR (100 MHz, $CDCl_3$): δ = 166.9, 154.2, 152.6, 136.7, 131.6, 129.2, 128.0, 123.2, 123.0, 59.6, 54.7, 40.4, 29.7, 29.6, 29.5, 29.3, 27.8, 27.1, 26.8, 25.9, 24.5; IR (neat): $\tilde{\nu}=3358$ (w), 2928 (s), 2851 (m), 2756 (w), 1639 (vs), 1537 (s), 1470 (m), 1296 (w), 1283 (w), 1275 (w), 1103 (m), 856 (s) cm^{-1}; UV-Vis ($CHCl_3$): λ_{max} (ε) = 326 (3.36×10^4), 447 nm (shoulder, 1.03×10^3 $mol^{-1}dm^3cm^{-1}$); HRMS (ESP+): *m/z* calcd for $C_{27}H_{38}N_4O$: 435.31184 $[M+H]^+$; found: 435.31176.

8: A solution of diazo acyl chloride **16** (29 mg, 0.09 mmol) in acetone (1.4 mL) was added to a solution of amine **18** (41 mg, 0.18 mmol) and K_2CO_3 (11 mg, 0.08 mmol) in H_2O (0.3 mL). The reaction mixture was stirred at room temperature for 19 h until the disappearance of **18** was assessed by a TLC control (DCM/MeOH/NH_4OH (6%) 10:1:0.1). The mixture was concentrated under vacuum and then the crude was purified by FCC in the dark (SiO_2, DCM/MeOH/NH_4OH (6%) 8:1:0.2) to give **8** (13 mg, 0.02 mmol, 20%) as an orange solid. $R_f=0.31$ (CH_2Cl_2:MeOH: NH_4OH (6%) 5:1:0.1); m.p. = 173–175 °C; ^{1}H NMR (400 MHz, $CDCl_3$): δ = 8.01–7.87 (m, 8H; Ar–H), 6.20 (t, $J=5.6$ Hz, 2H; N*H*), 3.48 (q, $J=6.8$ Hz, 4H; CH_2-15, CH_2-15′), 2.43-2.31 (m, 8H; CH_2-2, CH_2-2′, CH_2-6, CH_2-6′), 2.30–2.24 (m, 4H; CH_2-7, CH_2-7′), 1.69–1.55 (m, 12H; CH_2-3, CH_2-3′, CH_2-5, CH_2-5′, CH_2-14, CH_2-14′), 1.53–1.23 (m, 28H; CH_2-4, CH_2-4′, CH_2-8, CH_2-8′, CH_2-9, CH_2-9′, CH_2-10, CH_2-10′, CH_2-11, CH_2-11′, CH_2-12, CH_2-12′, CH_2-13, CH_2-13′); ^{13}C NMR (50 MHz, $CDCl_3$): δ = 166.8, 154.1, 137.3, 128.0, 123.3, 59.8, 54.8, 40.4, 29.8, 29.7, 29.6, 29.4, 27.9, 27.1, 27.1, 26.1, 24.6 Some carbons are missing due to overlap; IR (neat): $\tilde{\nu}=3312$ (m), 2922 (vs), 2851 (s), 2801 (w), 2764 (w), 1632 (vs), 1533 (vs), 1470 (m), 1290 (m) 1269 (m), 1155 (m), 1101 (m), 1011 (w), 860 (vs) cm^{-1}; UV-Vis ($CHCl_3$): λ_{max} (ε) = 332 (6.10×104), 443 nm (shoulder, 5.44×10^3 $mol^{-1}dm^3cm^{-1}$); HRMS (ESP+): *m/z* calcd for $C_{42}H_{66}N_6O_2$: 687.53200 $[M+H]^+$; found: 687.53250.

Biochemical characterization

Inhibitory activity towards human GCase from leukocyte homogenates. All experiments on biological materials were performed in accordance with the ethical standards of the institutional research committee and with the 1964 Helsinki Declaration and its later amendments. In keeping with ethical guidelines, all blood and cell samples were obtained for storage and analysed only after written informed consent of the

patients (and/or their family members) was obtained, using a form approved by the local Ethics Committee (Assigned code: Lysolate "Late -onset Lysosomal Storage Disorders (LSDs) in the differential diagnosis of neurodegenerative diseases: development of new diagnostic procedures and focus on potential pharmacological chaperones (PCs)." Project ID code: 16774_bio, 5 May 2020, Comitato Etico Regionale per la Sperimentazione Clinica della Regione Toscana, Area Vasta Centro, Florence, Italy). Control and patient samples were anonymized and used only for research purposes. Compounds were screened towards GCase at 1 mM in leukocytes isolated from healthy donors (controls). Isolated leukocytes were disrupted by sonication, and a micro-BCA protein assay kit (Sigma-Aldrich) was used to determine the total protein amount for the enzymatic assay, according to the manufacturer instructions. Enzyme activity was measured in a flat-bottomed 96-well plate. Compound solution (3 μL), 4.29 μg/μL leukocytes homogenate (7 μL), and substrate 4-methylumbelliferyl-β-D-glucopyranoside (3.33 mM, 20 μL, Sigma-Aldrich) in citrate/phosphate buffer (0.1 : 0.2, M/M, pH 5.8) containing sodium taurocholate (0.3%) and Triton X-100 (0.15%) were incubated for 1 h at 37 °C. The reaction was stopped by addition of sodium carbonate (200 μL; 0.5 M, pH 10.7) containing Triton X-100 (0.0025%), and the fluorescence of 4-methylumbelliferone released by GCase activity was measured in SpectraMax M2 microplate reader (λex = 365 nm, λem = 435 nm; Molecular Devices). For each compound a blank composed by a water solution containing 0.2% of bovine serum albumin (BSA), inhibitor and substrate (called "inhibitor blank") was tested and compared with the experiment blank, composed by BSA and substrate. No "inhibitor blank" differs from the experiment blank, demonstrating that the inhibitors do not interfere with the fluorescence of the hydrolyzed substrate. Percentage of GCase inhibition is given with respect to the control (without compound). Data are mean ± S.D. (n = 3). **IC_{50} determination**: The IC_{50} values of compounds **4s** (and *PSS*) and **5s** (and *PSS*) against GCase were determined by measuring the initial hydrolysis rate with 4-methylumbelliferyl-β-D-glucopyranoside (3.33 mM). Data obtained were fitted by using the appropriate Equation (for more details, see Supporting Information). **Kinetic Analysis**: The action mechanism of both compounds **4s** (and *PSS*) and **5s** (and *PSS*) was determined studying the dependence of the main kinetic parameters (Km and Vmax) from the inhibitor concentration. Kinetic data were analyzed using the Lineweaver-Burk plot (for more details, see Supporting Information).

Chaperoning activity assays. The effect of compounds **1**, **2**, **4s** (and *PSS*) and **5s** (and *PSS*)[17] on mutated GCase activity was evaluated in Gaucher patients' cells fibroblasts with the N370S/RecNcil or L444P/L444P mutations. Gaucher disease patients' cells were obtained from the "Cell line and DNA Biobank from patients affected by Genetic Diseases" (Gaslini Hospital, Genova, Italy). Fibroblasts cells (25×10^4) were seeded in T25 flasks with DMEM supplemented with fetal bovine serum (10%), penicillin/streptomycin (1%), and glutamine (1%) and incubated at 37 °C with 5% CO_2 for 24 h. The medium was removed, and fresh medium containing the iminosugar-based photoswitchable compounds was added to the cells and left for 4 days. The medium was removed, and the cells were washed with PBS and detached with trypsin to obtain cell pellets, which were washed four times with PBS, frozen and lysed by sonication in water. Enzyme activity was measured as reported above. Reported data are mean ± S.D. (n = 2).

Acknowledgements

MIUR - progetto Dipartimenti di Eccellenza2018–2022 (ref. B96C1700020008), Centro Interdipartimentale Risonanza Magnetica (C.I.R.M.), Universitá di Firenze and Fondazione CRF (project: MuTaParGa) Regione Toscana (Bando Salute 2018, project: Lysolate are acknowledged for financial support. P.M. and T.T. thanks Ministerio de Ciencia e Innovacion (Spain) (Project PID2019-104090RB-100) and Government of Aragón (Spain) (Grupos Consolidados, E34_20R) for financial support. The authors thankfully acknowledge the resources from the supercomputers "Memento" and "Cierzo", technical expertise and assistance provided by BIFI-ZCAM (Universidad de Zaragoza, Spain). F.C. thanks *i*DANEUROPARK for a postdoctoral fellowship. Open Access funding provided by Università degli Studi di Firenze within the CRUI-CARE Agreement.

Conflict of Interest

The authors declare no conflict of interest.

Data Availability Statement

The data that support the findings of this study are available in the supplementary material of this article.

Keywords: gaucher disease · glycomimetics · molecular dynamics · pharmacological chaperones · photoswitches

[1] F. M. Platt, A. D'Azzo, B. L. Davidson, E. F. Neufeld, C. J. Tifft, *Nat. Rev. Dis. Prim.* **2018**, *4*, 27.
[2] *Advances in Gaucher Disease: Gaucher Disease: Basic and Clinical Perspectives* (Ed.: G. A. Grabowski), Future Medicine, London, **2013**.
[3] For reviews on pharmacological chaperones for lysosomal storage disorders see: a) G. Parenti, *EMBO Mol. Med.* **2009**, *1*, 268–279; b) R. E. Boyd, G. Lee, P. Rybczynski, E. R. Benjamin, R. Khanna, B. A. Wustman, K. J. Valenzano, *J. Med. Chem.* **2013**, *56*, 2705–2725; c) M. Convertino, J. Das, N. V. Dokholyan, *ACS Chem. Biol.* **2016**, *11*, 1471–1489; d) D. M. Pereira, P. Valentão, P. B. Andrade, *Chem. Sci.* **2018**, *9*, 1740–1752; e) F. Chiti, J. W. Kelly, *Curr. Opin. Struct. Biol.* **2022**, *72*, 267–278.
[4] for reviews on pharmacological chaperones for gaucher diseases see: a) E. M. Sánchez-Fernández, J. M. García Fernández, C. Ortiz Mellet, *Chem. Commun.* **2016**, *52*, 5497–5515; b) J. M. Benito, J. M. García Fernández, C. Ortiz Mellet, *Expert Opin. Ther. Pat.* **2011**, *21*, 885–903; c) A. Trapero, A. Llebaria, *Future Med. Chem.* **2013**, *5*, 573–590; d) M. Martínez-Bailén, F. Clemente, C. Matassini, F. Cardona, *Pharmaceuticals* **2022**, *15*, 823–849.
[5] a) C. Kuriyama, O. Kamiyama, K. Ikeda, F. Sanae, A. Kato, I. Adachi, T. Imahori, H. Takahata, T. Okamoto, N. Asano, *Bioorg. Med. Chem.* **2008**, *16*, 7330–7336; b) Z. Luan, K. Higaki, M. Aguilar-Moncayo, H. Ninomiya, K. Ohno, M. I. García-Moreno, C. Ortiz Mellet, G. J. M. Fernández, Y. Suzuki, *ChemBioChem* **2009**, *10*, 2780–2792; c) M. I. García-Moreno, M. de la Mata, E. M. Sánchez-Fernández, J. M. Benito, A. Díaz-Quintana, S.

Fustero, E. Nanba, K. Higaki, J. A. Sánchez-Alcázar, J. M. García Fernández, et al., *J. Med. Chem.* **2017**, *60*, 1829–1842; d) T. Mena-Barragán, M. I. García-Moreno, A. Sevšek, T. Okazaki, E. Nanba, K. Higaki, N. I. Martin, R. J. Pieters, J. M. García Fernández, C. Ortiz Mellet, *Molecules* **2018**, *23*, 927; e) F. Clemente, C. Matassini, A. Goti, A. Morrone, P. Paoli, F. Cardona, *ACS Med. Chem. Lett.* **2019**, *10*, 621–626; f) F. Clemente, C. Matassini, C. Faggi, S. Giachetti, C. Cresti, A. Morrone, P. Paoli, A. Goti, M. Martínez-Bailén, F. Cardona, *Bioorg. Chem.* **2020**, *98*, 103740–103763; g) C. Vanni, F. Clemente, P. Paoli, A. Morrone, C. Matassini, A. Goti, F. Cardona, *ChemBioChem* **2022**, *23*, e202200077.

[6] a) N. Asano, K. Ikeda, L. Yu, A. Kato, K. Takebayashi, I. Adachi, I. Kato, H. Ouchi, H. Takahata, G. W. J. Fleet, *Tetrahedron: Asymmetry* **2005**, *16*, 223–229; b) C. Kuriyama, O. Kamiyama, K. Ikeda, F. Sanae, A. Kato, I. Adachi, T. Imahori, H. Takahata, T. Okamoto, N. Asano, *Bioorg. Med. Chem.* **2008**, *16*, 7330–7336; c) F. Stauffert, J. Serra-Vinardell, M. Gómez-Grau, H. Michelakakis, I. Mavridou, D. Grinberg, L. Vilageliu, J. Casas, A. Bodlenner, A. Delgado, P. Compain, *Org. Biomol. Chem.* **2017**, *15*, 3681–3705; d) T. Castellan, V. Garcia, F. Rodriguez, I. Fabing, Y. Shchukin, M. L. Tran, S. Ballereau, T. Levade, Y. Génisson, C. Dehoux, *Org. Biomol. Chem.* **2020**, *18*, 7852–7861.

[7] a) G. Parenti, G. Andria, K. J. Valenzano, *Mol. Ther.* **2015**, *23*, 1138–1148; b) J. Benz, A. C. Rufer, S. Huber, A. Ehler, M. Hug, A. Topp, W. Guba, E. C. Hofmann, R. Jagasia, R. M. Rodriguez Sarmiento, *Angew. Chem. Int. Ed.* **2021**, *60*, 5436–5442; *Angew. Chem.* **2021**, *133*, 5496–5502; c) M. Lan Tran, Y. Génisson, S. Ballereau, C. Dehoux, *Molecules* **2020**, *25*, 3145–3166.

[8] a) T. Mena-Barragán, A. Narita, D. Matias, G. Tiscornia, E. Nanba, K. Ohno, Y. Suzuki, K. Higaki, J. M. Garcia Fernández, C. Ortiz Mellet, *Angew. Chem. Int. Ed.* **2015**, *54*, 11696–11700; *Angew. Chem.* **2015**, *127*, 11862–11866; b) A. G. Santana, K. Robinson, C. Vickers, M. C. Deen, H.-M. Chen, S. Zhou, B. Dai, M. Fuller, A. B. Boraston, D. J. Vocadlo, L. A. Clarke, S. G. Withers, *Angew. Chem. Int. Ed.* **2022**, *61* (38), e202207974.

[9] M. G. Davighi, F. Clemente, C. Matassini, F. Cardona, M. B. Nielsen, A. Goti, A. Morrone, P. Paoli, M. Cacciarini, *Org. Biomol. Chem.* **2022**, *20*, 1637–1641.

[10] a) J. Daub, T. Knöchel, A. Mannschreck, *Angew. Chem. Int. Ed. Engl.* **1984**, *23*, 960–961; b) M. B. Nielsen, N. Ree, K. V. Mikkelsen, M. Cacciarini, *Russ. Chem. Rev.* **2020**, *89*, 573–586.

[11] a) A. A. Beharry, G. A. Woolley, *Chem. Soc. Rev.* **2011**, *40*, 4422–4437; b) W. A. Velema, W. Szymanski, B. L. Feringa, *J. Am. Chem. Soc.* **2014**, *136*, 2178–2191; c) J. Broichhagen, J. A. Frank, D. Trauner, *Acc. Chem. Res.* **2015**, *48*, 1947–1960; d) M. J. Fuchter, *J. Med. Chem.* **2020**, *63*, 11436–11447; e) A. Negi, C. Kieffer, A. S. Voisin-Chiret, *ChemistrySelect* **2022**, *7*, e202200981.

[12] A. Joosten, C. Decroocq, J. de Sousa, J. P. Schneider, E. Etam, A. Bodlenner, T. D. Butters, P. Compain, *ChemBioChem* **2014**, *15*, 309–319.

[13] C. Matassini, S. Mirabella, X. Ferhati, C. Faggi, I. Robina, A. Goti, E. M. Clavijo, A. J. M. Vargas, F. Cardona, *Eur. J. Org. Chem.* **2014**, 5419–5432.

[14] B. Soliman, N. Wang, G. Zagotto, S. Pockes, *Arch Pharm Chem Life Sci.* **2019**, *352*, 1900107–1900118.

[15] K. Rustler, S. Pockes, B. König, *ChemMedChem* **2019**, *14*, 636–644.

[16] A. Vlasceanu, M. Koerstz, A. B. Skov, K. V. Mikkelsen, M. B. Nielsen, *Angew. Chem.* **2018**, *130*, 6177–6180; *Angew. Chem. Int. Ed.* **2018**, *57*, 6069–6072.

[17] M. Incerti, L. Flammini, F. Saccani, G. Morini, M. Comini, M. Coruzzi, E. Barocelli, V. Ballabeni, S. Bertoni, *ChemMedChem* **2010**, *5*, 1143–1149.

[18] a) C. Matassini, J. Warren, B. Wang, A. Goti, F. Cardona, A. Morrone, M. Bols, *Angew. Chem. Int. Ed. Engl.* **2020**, *59*, 10466–10469; b) M. Martínez-Bailén, A. T. Carmona, A. C. Patterson-Orazem, R. L. Lieberman, D. Ide, M. Kubo, A. Kato, I. Robina, A. J. Moreno-Vargas, *Bioorg. Chem.* **2019**, *86*, 652–664.

[19] a) M. G. Davighi, F. Clemente, C. Matassini, A. Morrone, A. Goti, M. Martínez-Bailén, F. Cardona, *Molecules* **2020**, *25*, 4526; b) F. Clemente, C. Matassini, S. Giachetti, A. Goti, A. Morrone, M. Martinez-Bailén, S. Aorta, P. Merino, F. Cardona, *J. Org. Chem.* **2021**, *86*, 12745–12761.

[20] For some reviews on multivalency effect, see: a) P. Compain, A. Bodlenner, *ChemBioChem* **2014**, *15*, 1239–1251; b) S. G. Gouin, *Chem. Eur. J.* **2014**, *20*, 11616–11628; c) R. Zelli, J.-F. Longevial, P. Dumy, A. Marra, *New J. Chem.* **2015**, *30*, 5050–5074; d) C. Matassini, C. Parmeggiani, F. Cardona, A. Goti, *Tetrahedron Lett.* **2016**, *57*, 5407–5415; e) P. Compain, *Chem. Rec.* **2020**, *20*, 10–22; f) M. González-Cuesta, C. Ortiz Mellet, J. M. García Fernández, *Chem. Commun.* **2020**, *56*, 5207–5222.

[21] C. Parmeggiani, S. Catarzi, C. Matassini, G. D'Adamio, A. Morrone, A. Goti, P. Paoli, F. Cardona, *ChemBioChem* **2015**, *16*, 2054–2064.

[22] a) G. R. Bowman, E. R. Bolin, K. M. Hart, B. C. Maguire, S. Marqusee, *PNAS* **2015**, *112*, 2734–2739; b) N. Wu, L. Strömich, S. N. Yaliraki, *Patterns* **2022**, *3*, 100408.

[23] J. Benz, A. C. Rufer, S. Huber, A. Ehler, M. Hug, A. Topp, W. Guba, E. C. Hofmann, R. Jagasia, R. M. Rodríguez Sarmiento, *Angew. Chem. Int. Ed.* **2021**, *60*, 5436–5442; *Angew. Chem.* **2021**, *133*, 5496–5502.

[24] J. Zheng, L. Chen, O. S. Skinner, D. Ysselstein, J. Remis, P. Lansbury, R. Skerlj, M. Mrosek, U. Heunisch, S. Krapp, J. Charrow, M. Schwake, N. L. Kelleher, R. B. Silverman, D. Krainc, *J. Am. Chem. Soc.* **2018**, *140*, 5914–5924.

[25] R. L. Lieberman, B. A. Wustman, P. Huertas, A. C. Powe Jr., C. W. Pine, R. Khanna, M. G. Schlossmacher, D. Ringe, G. A. Petsko, *Nat. Chem. Biol.* **2007**, *3*, 101–107.

[26] T. Halgren, *Chem. Biol. Drug Des.* **2007**, *69*, 146–148. Schrödinger Release 2021–4: SiteMap, Schrödinger, LLC, New York, NY, **2021**.

[27] R. A. Friesner, J. L. Banks, R. B. Murphy, T. A. Halgren, J. J. Klicic, D. T. Mainz, M. P. Repasky, E. H. Knoll, M. Shelley, J. K. Perry, D. E. Shaw, P. Francis, P. S. Shenkin, *J. Med. Chem.* **2004**, *47*, 1739–1749.

Manuscript received: December 8, 2022
Accepted manuscript online: January 4, 2023
Version of record online: March 1, 2023